# Open Archive Toulouse Archive Ouverte (OATAO)

OATAO is an open access repository that collects the work of Toulouse researchers and makes it freely available over the web where possible.

# Investigations into the coefficient of thermal expansion of porous films prepared on AA7175 T7351 by anodizing in sulphuric acid electrolyte

Yann Goueffon [a], Catherine Mabru [b,*], Michel Labarrère [b], Laurent Arurault [c], Claire Tonon [d], Pascale Guigue [a]

[a] CNES, 18 avenue Edouard Belin, 31401 Toulouse Cedex 9, France
[b] Université de Toulouse, ISAE, Institut Clément Ader, 10 avenue Edouard Belin, BP 54032, 31055 Toulouse Cedex 4, France
[c] Université de Toulouse, CIRIMAT, UPS/INPT/CNRS, LCMIE, Bat 2R1, 118 route de Narbonne, 31062 Toulouse Cedex 9, France
[d] EADS ASTRIUM Satellites, 31 avenue des Cosmonautes, 31402 Toulouse Cedex 4, France

## ABSTRACT

The aim of this study was to investigate the Coefficient of Thermal Expansion (CTE) of anodic films on 7175 T7351 aluminium alloy and to evaluate the influence of the film characteristics on this value. In particular, effects of porosity and post-treatments, such as coloring and sealing, were studied. Beam bending analysis was used as the experimental method and a numerical finite element model was developed to verify theoretical relationships hypotheses. In particular, the errors induced by the use of theoretical relationships between the curvature of the sample and stresses in the film were not negligible. A relation based on a finite element model was then developed and used to calculate stresses. The experimental value of CTE obtained by beam bending test was then validated by comparing the experimental cracking temperature of anodic films with a theoretical value directly depending on the previously determined CTE.
The CTE of anodic films was found to be $13.0 \pm 1.0 \ 10^{-6} \ K^{-1}$ independent from the porosity of the films and from the post-treatment (inorganic coloring and sealing).

## 1. Introduction

Anodic films are processed on light alloys to obtain specific superficial characteristics. Actually, the growth of oxide films increases for example the surface hardness, [1] the corrosion resistance [2] or the wear resistance [3]. Post-treatments of the coating are available either to add specific properties or to improve existing ones.

For instance, the coloring of anodic films constitutes a potential post-treatment. It can be realized by electrolytic process [4–6] or by impregnation of organic [7] or inorganic [8–11] dyes inside its pores. This treatment is often processed for esthetic purpose [12] but sometimes also to provide specific thermo-optical properties [9–11].

A second example of post-treatment is sealing. The simplest method is an immersion in boiling water. The hydration of the aluminium oxide results in a volume expansion of the film and closes the pores [13]. Additives in the sealing bath are sometimes used to increase the efficiency of the treatment. For example, an additional precipitation of protective nickel hydroxide on the film is obtained by introduction of nickel acetates in the bath [14,15]. The sealing can be processed on a non-colored film; its corrosion resistance is then enhanced. But it can also be realized on a colored film to maintain and protect dyes from the external environment [16].

The differential thermal dilatations between the substrate and the film can lead to the crazing of the film when thermally loaded [17]. Coefficient of Thermal Expansion (CTE) of bulk materials is easily measured by dilatometry and is known for a large range of materials. Nevertheless, thin films are much more difficult to characterize. For aluminium alloys, it is reported in the literature that the CTE of anodic films measured by dilatometry is about $5 \times 10^{-6} \ K^{-1}$ [18]. Even if details on the experimental method employed to determine this value are not available, it has been used in numerous publications [17,19,20]. Nevertheless, more recently, Zhou et al. [21] used X-ray diffraction to evaluate the CTE of anodic films under partially crystallized powder form (no influence of the substrate). They found a value of $14.1 \times 10^{-6} \ K^{-1}$ and explained the difference from previous results by the impact of residual stresses on the CTE when the substrate is present.

In this context, the present study aims to determine the CTE of anodic films still supported on a 7XXX aluminium alloy. Because it was previously shown that these films are in fact amorphous [22], measurements have been performed using the curvature technique. Under thermal loading, the deformation mismatch of a coating on a thin substrate (approximately ten times thicker than coating) induces a curvature of the sample. The measurement of this curvature allows the calculation of film stresses which are related to the coefficients of thermal expansion of both film and substrate. Knowing the CTE of the substrate, the CTE of the film can then be evaluated.

* Corresponding author. Tel.: +33 561 339 150; fax: +33 561 339 095.
*E-mail address:* Catherine.mabru@isae.fr (C. Mabru).

A numerical finite element model has been developed to discuss the relationship between film stresses and curvature on the one hand, and the relationship between film stresses and temperature on the other hand.

Validation of the CTE was carried out by comparing the predicted cracking temperature with experimental results in the case of anodic films without any post-treatment. Finally, the influence of post-treatments (such as coloring and sealing) on this property was investigated, which has never been studied before to our knowledge.

## 2. Experimental methods

### 2.1. Material and samples geometry

The aluminium substrate was an AA7175 T7351 often used in the space industry. Its Young's modulus is known to be $E_s = 72$ GPa, its Poisson's ratio $\nu_s = 0.33$ and its CTE $\alpha_s = 23.6 \ 10^{-6} \ K^{-1}$ [23]. The size of the samples before any surface treatments was $40 \ mm \times 20 \ mm \times 200 \ \mu m$. To obtain this thickness, a rolled aluminium sheet of 7 mm was milled until 3 mm. The thickness of 200 μm was then obtained by mechanical polishing. The final step of the polishing was done with a ¼ μm diamond powder. The planarity of the sample was verified with a profilometer at this step. These samples were then anodized on one side according to the following process.

### 2.2. The black anodizing process

The black anodizing process used followed the ESA standard [24] for spacecraft design. It consists of four main steps: pretreatments, anodizing, inorganic coloring and sealing.

The aluminium sheets were degreased with ethanol, etched in an aqueous mixed solution of $Na_2CO_3/Na_3PO_4$ for 5 min at 93 °C and neutralized 3 min at room temperature in $HNO_3$ (50 %v/v). The samples were rinsed with distilled water at the end of each step.

The anodizing parameters were extensively studied elsewhere [10,15,25] in order to obtain a thickness ($20 \pm 3 \ \mu m$) meeting the ESA requirements [24]. Samples were anodized during 60 min in a sulphufic acid bath (150 g/L) with a current density of 1.25 A/dm². A thermo-regulated cell was used in the present study, while the manufacturers usually leave the electrolyte at room temperature. The temperature was set here at 5 °C, 10 °C, 15 °C or 20 °C to adjust the initial porosity at 10%, 20%, 30% or 40% respectively. To evaluate the porosity, the surface of the anodic films was observed using Field Emission Gun-Scanning Electron Microscopy (FEG-SEM JEOL JSM 6700F) and the resulting images were analysed with the free software ImageJ. The ratio between the pore areas and the total surface area analysed was taken to be the porosity of the anodic film, i.e. the porosity was considered homogeneous through the whole thickness of the anodic film [15].

The anodized parts were colored by immersion in two different baths. Firstly a solution of cobalt acetate (200 g/L) at 43 °C was used to fill in the pores for 15 min. Secondly, an immersion in ammonium sulphide (30 g/L) at room temperature for 10 min resulted in the precipitation of black dyes (CoS) in the pores. Whatever the initial porosity, the dyes were mainly present at the surface of the film [15].

The next step was to seal the parts in an aqueous solution of nickel acetate (5 g/L) and boric acid (5 g/L) at $98 \pm 2$ °C. The hydration of the oxide is used to close pores and protect dyes. Finally, the samples were carefully rinsed using deionized water.

### 2.3. Mechanical characteristics of the films

The Young's modulus of uncolored and unsealed films is homogenous and directly linked to the porosity (p) through Wang's law [15]: $E = E_0 \exp(-(bp + cp^2))$ with ($E_0 = 86.2$ GPa; $b = 0.2$; $c = 2.48$).The coloring and sealing steps generate a decrease of this modulus only at the surface of the film resulting in a gradient of modulus across the thickness [15].

Different values of Poisson's ratio have been used for anodic films: for example 0.24 by Zhou et al. [21], or 0.25 by Nelson and Oriani [26]. In this study we have chosen $\nu_f = 0.28$ [27]; the choice of this value has a negligible effect on the calculated values that follow. In addition, the increase of porosity may have no impact on this Poisson's ratio as it has been observed on α alumina [28].

### 2.4. Relationships between the stresses in the film and the curvature of the sample

When the ratio between the thickness of the substrate ($t_s$) and the thickness of the film ($t_f$) is low enough, the presence of stresses in the film generates a curvature of the sample. Stoney [29] proposed a relationship (1) to link the stresses in the film ($\sigma_f$) to the radius of curvature (R) of the sample.

$$\sigma_f = \frac{E_s t_s^2}{6Rt_f} \tag{1}$$

The relationship uses the Young's modulus of the substrate $E_s$. Campbell [30] integrated the Poisson's ratio of the substrate $\nu_s$ in the equation and proposed the following relationship (2).

$$\sigma_f = \frac{E_s t_s^2}{6R(1-\nu_s)t_f} \tag{2}$$

More recently, Yan [31] proposed a relationship (3) to take into account a difference of Young's modulus between the film ($E_f$) and the substrate ($E_s$):

$$\sigma_f = \frac{E_f t_f}{6R(1-\nu_f)} \frac{1 + 4\gamma\beta + 6\gamma^2\beta + 4\gamma^3\beta + \gamma^4\beta^2}{(1+\gamma)(1+\gamma\beta)} \quad \gamma = \frac{t_s}{t_f} \quad \beta = \frac{E_s(1-\nu_f)}{E_f(1-\nu_s)} \tag{3}$$

In these three equations, the stresses are assumed to be homogeneous in the film and the thickness of the film is considered to be much lower than that of the substrate. It can also be noted that other relationships have been developed to take into account the anisotropy of the film for example [32]. However, due to the spongy morphology of anodic films in the present case [10], isotropic behavior has been assumed in the following study.

### 2.5. Evaluation of the coefficient of thermal expansion of the film (CTE)

The curvature of thin samples was evaluated with a profilometer «Mahr Perthometer». It was first verified that the contact strength between the probe and the sample does not modify the curvature significantly. At room temperature, the curvature measured is representative of residual stresses in the film, due to the process. The sample was then warmed with a heating stage until 100 °C with heating/cooling rate of 10 °C/min. The temperature was monitored by a thermocouple directly on the surface of the sample. Differential dilatations between the film and the substrate generate additional stresses in the film and modify the curvature. By measuring the curvature at different temperatures, an experimental relationship between the stresses in the film ($\sigma_f$) and the temperature (θ) is obtained.

Using the theoretical Eq. (4) [21,33], the unknown coefficient of thermal expansion of the film ($\alpha_f$) can be determined by simply evaluating the slope of the experimental curve obtained.

$$\Delta\sigma_f = \frac{E_s}{(1-\nu_s)} \frac{(\alpha_s - \alpha_f)}{m + \frac{1}{n}} \Delta\theta \quad \text{with } m = \frac{t_f}{t_s} \quad \text{and } n = \frac{\frac{E_f}{1-\nu_f}}{\frac{E_s}{1-\nu_s}} \tag{4}$$

Variations of the Young's modulus with the temperature are here neglected [34], and the film thickness is also assumed to be much lower than that of the substrate.

## 2.6. Numerical model

A finite element model was used to verify the validity of the previous Eqs. (1–3: Stress vs. Curvature; 4: Stress vs. Temperature) when the ratio of thickness $t_s/t_f$ is about ten as obtained on the samples of the present study. A 2D-model, composed of a thin film on its substrate, was developed for each sample studied. The geometry of the model and the material properties (especially the film modulus) were modified to adjust them to the different samples. The only unknown parameter is the CTE of the film. The software SAMCEF was used to perform isotropic thermo-elastic calculations with 2-dimensional plane strain hypotheses.

Thermal loadings were applied uniformly and constantly. The stresses in the film ($\sigma_f$) and the curvature (R) of the numerical model were analyzed.

First, a finite element law $\sigma_f = f$ (R) was obtained for each sample geometry and compared with the theoretical relationships 2 (Campbell) and 3 (Yan).

Secondly, a finite element law $\sigma_f = f$ ($\theta$) was obtained and compared to Eq. (4).

## 2.7. Validation of CTE measurements

Values of CTE have been validated by comparing the theoretical cracking temperature to the experimental results. Actually, according to Eq. (4), cracking temperature ($\theta_{critical}$) is directly dependent on the film CTE and films properties (5).

$$\sigma_m - \sigma_{residual} = \frac{E_s}{1 - \nu_s} \frac{\left(\alpha_s - \alpha_f\right)}{m + \frac{1}{n}} (\theta_{critical} - \theta_{ambient}) \tag{5}$$

The cracking stress $\sigma_{cracking}^{applied}$ is defined as the tensile stress leading to crack initiation (6) and is the difference between the failure tensile stress ($\sigma_m$) and residual stress ($\sigma_{residual}$) of the film.

$$\sigma_{cracking}^{applied} = \sigma_m - \sigma_{residual} \tag{6}$$

This cracking stress was evaluated by four-point bending monitored by acoustic emission (Fig. 1). The anodic film is then placed under uniform tensile stresses. The cracking load ($F_c$) of the film is detected by acoustic emission. The detection threshold was fixed at 50 dB and we verified that this detected signal was only due to the film damage. Actually, tests with samples without anodizing treatment were performed to verify that acoustic emissions due to plastic deformations are totally filtered with this threshold. By assuming that strains of the films are imposed by the substrate (no sliding) and that the film is purely elastic, the applied cracking stress can be calculated (7) as a function of the critical load applied ($F_c$):

$$\sigma_m - \sigma_{residual} = E_f \frac{F_c a h}{4 I_s E_s} \tag{7}$$

$I_s$ is the quadratic moment of the substrate, while $a$ and $h$ are sample dimensions as defined on Fig. 1.
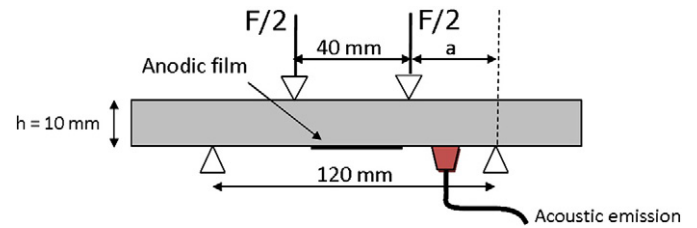


**Fig. 1.** Diagram of the four-point bending test monitored by acoustic emission.

By combining 5 and 7 this critical temperature can be expressed (8) as a function of $F_c$ (obtained by four-point bending) and $\alpha_f$.

$$\theta_{critical}^{theoretical} = \frac{E_f \frac{F_c a h}{4 E_s I_s}}{\frac{E_s}{1 - \nu_s} \frac{\left(\alpha_s - \alpha_f\right)}{m + \frac{1}{n}}} + \theta_{ambient} \quad \text{with } m = \frac{t_f}{t_s} \quad \text{and} \quad n = \frac{\frac{E_f}{1 - \nu_f}}{\frac{E_s}{1 - \nu_s}} \tag{8}$$

An experimental value of the critical temperature leading to cracks initiation was obtained by observation of a sample heated (Philips FP6752, 1000 °C Heating Stage System) inside a Scanning Electron Microscope (Philips XL30 ESEM). The thickness of the substrate was here 1 mm to avoid bending of the sample. The heating rate was 10 °C/min and the temperature was controlled with a thermocouple placed under the sample.

A validation of the CTE was thus obtained by comparing the experimental and the theoretical values of the cracking temperatures.

## 3. Results and discussion

### 3.1. Hypotheses validation

#### 3.1.1. Film stresses vs. curvature

In the relationships of Campbell and Yan the stress in the film is directly proportional to the curvature (1/R) of a thin sample. The use of the numerical model confirms this tendency. A linear relationship between the stress and the curvature (linear regression $R^2 = 1$) was also obtained by applying different thermal loadings to samples. Thus, a new "Finite Element Model (FEM) relationship" can be written as (9):

$$\sigma_f = \frac{K\left(E_s, E_f, t_s, t_f\right)}{R} \tag{9}$$

This relationship is adapted to the geometry of the considered sample. When $E_f = E_s$ and $t_s/t_f > 30$ the results obtained by the three relationships are very close. Nevertheless, as seen on Fig. 2 differences appear when the thickness ratio decreases ($t_s/t_f = 10$ for Fig. 2). In such a case, the curvature of the sample induces a partial release of the film stresses which is underestimated in Campbell and Yan laws. It is also confirmed on Fig. 2 that the choice of the film CTE has no impact on the FEM relationship. Actually, the relationship between stress in the film and curvature does not depend on the loading mode.

Samples of the present study have a thickness ratio about 10, so the FEM relationship seems better adapted to our experimental technique.

#### 3.1.2. Film stresses vs. temperature

Eq. (4) gives the stresses in the film due to the differential thermal dilatations. Nevertheless, one of the hypotheses of this equation is also that the film is considered much thinner than the substrate. In order to verify the validity of the relationship, thermo-mechanical calculations were performed and an error was defined by the Eq. (10):

$$Error = \frac{\sigma_{relation4} - \sigma_{FEM}}{\sigma_{FEM}} \tag{10}$$
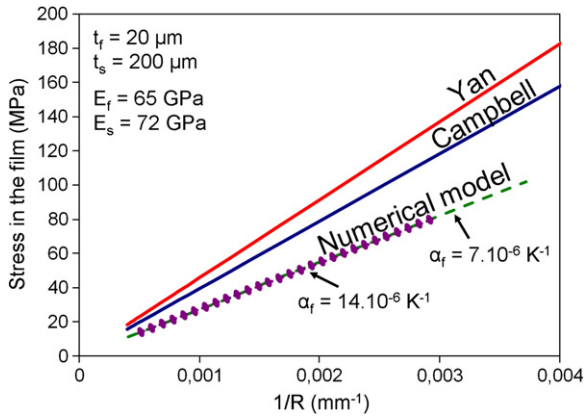
**Fig. 2.** Comparison between Campbell's law, Yan's law and the relationship obtained with the finite element model for a thickness ratio (substrate/film) of ten.

The evolution of the error as a function of the thickness ratio (for $E_f = 50$ GPa and $T = 80$ °C) can be observed on Fig. 3. Error is lower than 7% and decreases when the ratio increases. When the thickness ratio is ten, the error is lower than 10% for the conditions met in experimental techniques (a temperature range of 20 °C/100 °C and a Young's modulus of the film lower than 80 GPa). Eq. (4) will thus be used later in this study assuming that this error is acceptable.

### 3.2. Films not colored and not sealed

#### 3.2.1. Beam bending measurements of CTE

The CTE has first been studied in the case of anodic films not colored and not sealed. Fig. 4 shows the evolution of the curvatures of thin samples with changes of temperature. The porosity of the film is 30% in this example. The curves presented on Fig. 5 are then obtained by using the three relationships compared previously. It can be observed that compressive residual stresses become tensile when the temperature increases. The behavior of samples was identical during the heating and the cooling phases. The slope of each curve was measured and the Eq. (4) allowed identifying the CTE of the film.

Campbell and Yan relationships lead respectively to values $\alpha_f^{Campbell} = 6.5 \pm 1.0\ 10^{-6}\ K^{-1}$ and $\alpha_f^{Yan} = 4.0 \pm 1.0\ 10^{-6}\ K^{-1}$. Those values are close to $5.10^{-6}\ K^{-1}$ often used in the literature [18–20].

However, the FEM relationship, better adapted to the geometry of samples, results in a coefficient of thermal expansion of the film $\alpha_f^{FEM} = 13.0 \pm 1.0\ 10^{-6}\ K^{-1}$. This value is close to the one determined recently by Zhou et al. [21] ($14.1\ 10^{-6}\ K^{-1}$).

Table 1 summarises $\alpha_f^{FEM}$ values determined for anodic films before coloring and sealing as a function of their porosity. Each time, a numerical model with the geometry and a film modulus corresponding to the tested sample was developed to obtain the proportionality coefficient between stresses in the film and curvature ($K(E_s, E_f, t_s, t_f)$).
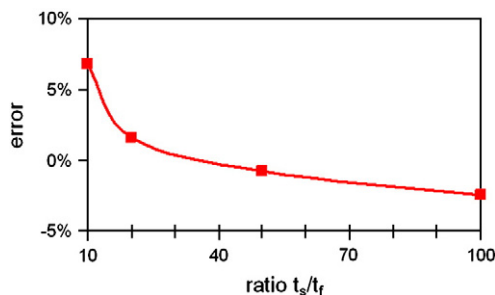


**Fig. 3.** Evolution of the error between Eq. (4) and results obtained by the numerical model as a function of the thickness ratio ($E_f = 50$ GPa, $T = 80$ °C and $\alpha_f = 5.10^{-6}\ K^{-1}$).
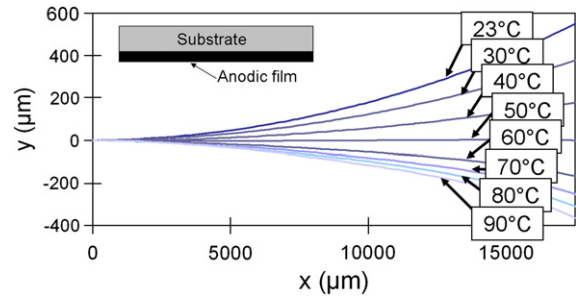


**Fig. 4.** Evolution of the profile of a thin sample with temperature variations (anodic film not colored and not sealed with a porosity of 30%).

Thus the coefficient of thermal expansion is independent of the porosity of the film and its average value is $\alpha_f = 13.0\ 10^{-6}\ K^{-1}$.

#### 3.2.2. Validation of the CTE

Cracking temperature measurements were performed to validate the CTE of anodic film determined previously. The critical strength has been measured during the four-point bending test for anodic films with different porosities (Fig. 6). Knowing these values, the theoretical temperature of cracking (Relation 8) of each sample is only dependent on one unknown parameter: the CTE of the film.

The cracking temperature was then evaluated by heating in an electronic microscope. For example, we can evaluate the cracking temperature of an anodic film 20% of porosity at $270 \pm 10$ °C (Fig. 7).

The comparison between the theoretical and experimental cracking temperatures is presented on Fig. 8. Whatever the porosity, these measures confirm that the CTE is about $13.10^{-6}\ K^{-1}$. A value of $5.10^{-6}\ K^{-1}$ would have led to cracking temperatures nearly half as much. This validates the experimental beam bending analysis used.

### 3.3. Films colored and not sealed

#### 3.3.1. Influence of the gradient of modulus on the film stress state

Before the coloring step, we proved in a previous study [15] that the composition and the mechanical properties (especially the young modulus) of films are homogenous with the thickness. However, once colored, dyes are mainly located at the top of the film, generating a gradient of Young's modulus [15] and potentially of internal stresses.

The previous calculations of Section 3.1.1 were made with a uniform averaged modulus. Actually, the curvature method only gives information on the average stress in the film. A numerical model with a gradient of modulus was realized and its behavior seems very close to the model with a uniform modulus (Fig. 9). Thus, the FEM relationship is not significantly affected by the modulus gradient of
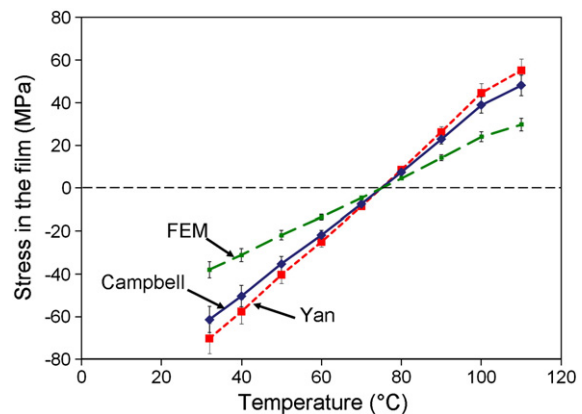


**Fig. 5.** Stresses in the film as a function of the temperature calculated with the three different laws (anodic film not colored and not sealed with a porosity of 30%).

**Table 1**
Evolution of the CTE of anodic films before and after coloring as a function of their porosity.

| Porosity | 10% | 20% | 30% | 40% |
|---|---|---|---|---|
| $\alpha_f^{FEM}$ ($10^{-6}$ K$^{-1}$) before coloring | 13.4 ± 1.0 | 12.9 ± 1.0 | 13.0 ± 1.0 | 12.2 ± 1.0 |
| $\alpha_f^{FEM}$ ($10^{-6}$ K$^{-1}$) after coloring | 14.9 ± 3.0 | 10.3 ± 3.0 | 16.2 ± 3.0 | Not measurable |
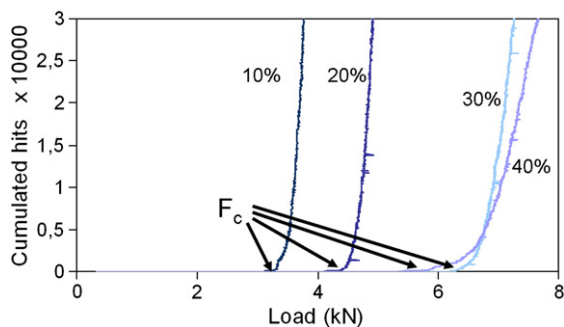


**Fig. 6.** Detection of acoustic signals during four-point bending test in the case of anodic films with different initial porosities.

the studied samples and the previous model with uniform modulus will be used in the following.

### 3.3.2. Beam bending measurement of the CTE

Curvature measurements at room temperature show positive residual stress after coloring of the anodic film. The evolution of film stress was identical again during heating and cooling. Table 1 shows that this coloring does not modify the CTE of the film. Measurements were not possible at 40% of initial porosity because films were crazed after the coloring step [15] and internal stresses were thus partially released.

### 3.4. Films colored and sealed

As seen previously, the curvature after cooling is the same as before heating for samples not sealed (colored or not). In this case, the test has no influence on the stresses in the film at room temperature.

On the contrary, samples colored and sealed have an initial compressive residual stress while the stress after heating and cooling is positive (Fig. 10). The initial compressive stresses are due to the volume expansion generated by the hydration of the film during the sealing step. Dehydration occurs around 100 °C and a release of these hydration stresses is observed. During the cooling the behavior of the film becomes equivalent as the one of films colored but not sealed. Fig. 10 presents the case of a film with 10% of initial porosity but same observations were done for 20% of porosity. Cracks were present in sealed films with higher porosities thus the evaluation of stresses was not possible.

The slopes during heating and cooling are comparable (for temperatures lower than 80 °C) thus the CTE of the film is not significantly modified by the sealing step.

## 4. Conclusion

The aim of this study was to investigate anodic films CTE and to observe the influence of the porosity—an important film characteristic
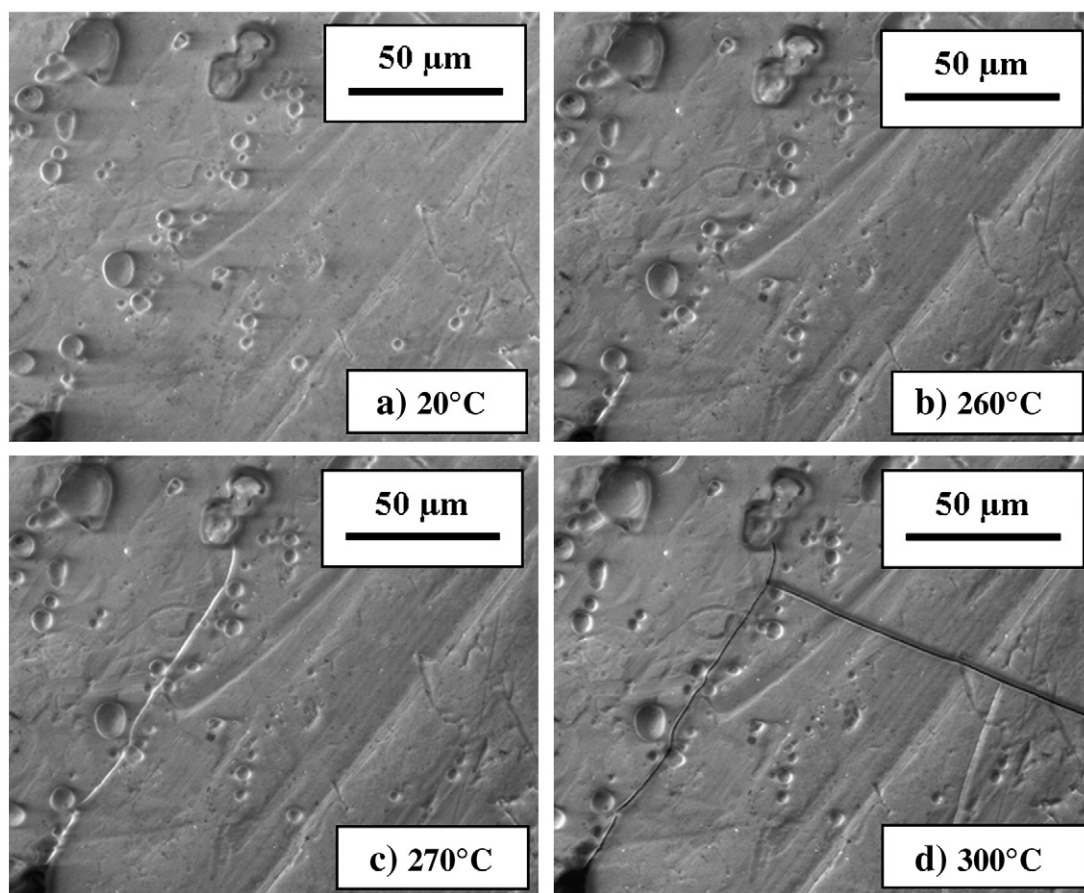


**Fig. 7.** SEM surface observation of anodic films (20% of porosity) at different temperatures (a: 20 °C; b: 260 °C; c: 270 °C and d: 300 °C).
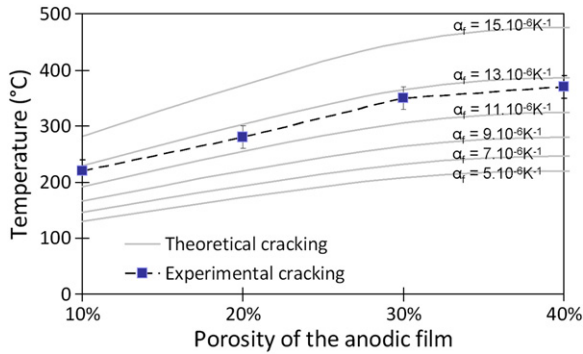
**Fig. 8.** Experimental and theoretical cracking temperatures of anodic films with different porosities.
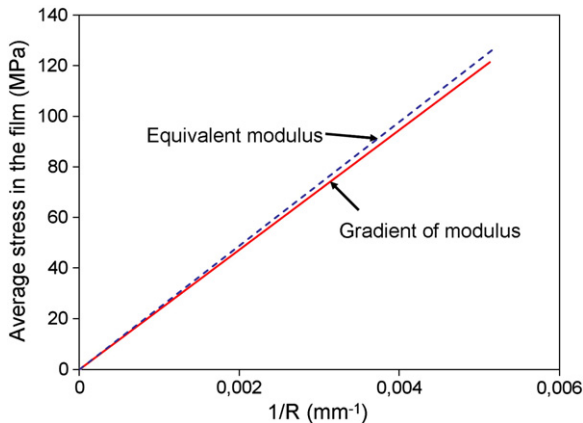


**Fig. 9.** Relationship between average stress in the film and curvature of the sample obtained by FEM for an average uniform modulus or a gradient of modulus.
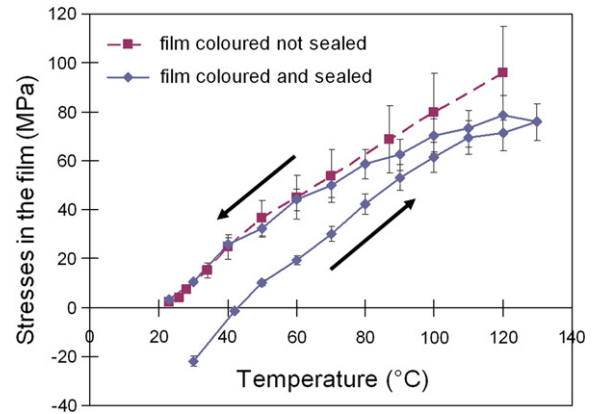


**Fig. 10.** Evolution of the stresses in the film during heating and cooling for a sealed and non-sealed colored film (10% of initial porosity).

—on this value. In addition, effects of post-treatments such as coloring and sealing were also studied.

Beam bending analysis was developed as the experimental method to evaluate the CTE of anodic films. In particular, the validity of theoretical relationships was verified using a Finite Element Model whose geometry is representative of experimental samples. It was thus shown that theoretical relationships between stress in the film and curvature sample that were found in the literature, were not valid for the present study and a new relationship was established using this numerical model. The validity of the CTE values obtained, and thus of the measurement method used, was confirmed by measuring the cracking temperature of anodic films and comparing it with the theory.

The coloring step has been proved to have no influence on the CTE of anodic films. Until this step, no influence of an eventual dehydration on the mechanical behavior is observed. On the contrary, the compressive internal stresses induced during the sealing step are released when the film is heated. From a purely mechanical point of view, the hydration of the film is thus a reversible phenomenon. CTE values are not affected by the sealing step.

The CTE of anodic films realized on 7175 T7351 was evaluated to be $13.0 \pm 1.0 \ 10^{-6} \ \mathrm{K}^{-1}$. In addition, it has been shown that this value is independent of the porosity of the film. This result is in contradiction with several authors [18–20] who used a value of $5 \ 10^{-6} \ \mathrm{K}^{-1}$ but close to investigations realized by Zhou [21] who concluded a CTE of 14.1 $10^{-6} \ \mathrm{K}^{-1}$.

## References

[1] G. Alcala, S. Mato, P. Skeldon, G.E. Thompson, A.B. Mann, H. Habazaki, K. Shimizu, Surf. Coat. Technol. 173 (2003) 293.
[2] M. Garcia-Rubio, M.P. de Lara, P. Ocon, S. Diekhoff, M. Beneke, A. Lavia, I. Garcia, Electrochim. Acta 54 (2009) 4789.
[3] T. Aerts, Th. Dimogerontakis, I. De Graeve, J. Fransaer, H. Terryn, Surf. Coat. Technol. 201 (2007) 7310.
[4] L. Arurault, J. Salmi, R.S. Bes, Sol. Energ. Mat. Sol. C. 82 (2004) 447.
[5] L. Arurault, G. Zamora, V. Vilar, P. Winterton, R. Bes, J. Mater. Sci. 45 (2010) 2611.
[6] H.H. Shih, Y.C. Huang, J. Mater. Process. Tech. 208 (2008) 24.
[7] S. Wernick, R. Pinner, P.G. Sheasby, The surface treatment and finishing of aluminium and its alloys, Fifth Edition, Vol.2, Finishing Pub. LTD&ASM Intert. Ed, Teddington-England, 1987, p. P.730.
[8] R. LeVesque, M. Ho, B. Vickers, H. Babel, A. Pard, AIAA-92-2160-CP, In AAIA Technical papers (A92-31285 12-23) Washington, USA, 1992, p. 56.
[9] A. Scherer, O.T. Inal, Thin Solid Film 101 (1983) 311.
[10] Y. Goueffon, L. Arurault, C. Mabru, C. Tonon, P. Guigue, J. Mater. Process. Tech. 209 (2009) 5145.
[11] C. Siva Kumar, S.M. Mayanna, K.N. Mahendra, A.K. Sharma, R. Uma Rani, Appl. Surf. Sci. 151 (1999) 280.
[12] L. Arurault, Actual. Chim. 327–328 (2009) 45.
[13] V. Lopez, E. Otero, E. Escudero, J.A. Gonzalez, Surf. Coat. Technol. 154 (2002) 34.
[14] L. Hao, B.R. Cheng, Met. Finish. 98 (2000) 8.
[15] Y. Goueffon, L. Arurault, S. Fontorbes, C. Mabru, C. Tonon, P. Guigue, Mat. Phys. Chem. 120 (2010) 636.
[16] J.W. Diggle, T.C. Downie, C.W. Goulding, Chem. Rev. 69 (1969) 365.
[17] X. Zhao, W. Liu, Y. Zuo, L. Yang, J. Alloy. Comp. 479 (2009) 473.
[18] S. Wemick, R. Pinner, The Surface Treatment and Finishing of Alumimum and its Alloys, 4th Ed, Robert Draper Ltd, Teddington, 1972, p. p.508.
[19] R.S. Alwitt, R.C. McClung, Plat. Surf. Finish. 80 (1993) 48.
[20] R.C. McClung, R.S. Alwitt, ASTM STP 1184, American society for Testing, Materials, Philadelphia, 1994, p. 156.
[21] J. Zhou, J. Wu, Y. Yang, Thin Solid Films 346 (1999) 280.
[22] S. Ono, H. Ichinose, T. Kawaguchi, N. Masuko, Corros. Sci. 31 (1990) 249.
[23] J.R. Davis, ASM Specialty Handbook: Aluminum and Aluminum Alloys, Ed. ASM International, Materials Park, Ohio, USA, 1993, p. 73.
[24] ECSS-Q-70-03A – Norme ESA, Black-anodizing of metals with inorganic dyes, http://www.ecss.nl 2006.
[25] Y. Goueffon, C. Mabru, M. Labarrere, L. Arurault, C. Tonon, P. Guigue, Surf. Coat. Tech. 204 (2009) 1013.
[26] J.C. Nelson, R.A. Oriani, Corros. Sci. 34 (1993) 307.
[27] R.S. Alwitt, J. Xu, R.C. McClung, J. Electrochem. Soc. 140 (1993) 1241.
[28] M. Asmani, C. Kermel, A. Leriche, M. Ourak, J. Eur. Ceram. Soc. 21 (2001) 1081.
[29] G.G. Stoney, Proc. R. Soc. Lond. 82 (1909) 172.
[30] D.S. Campbell, Mechanical Properties of Thin Films, chapter 12, McGraw-Hill, New York, 1970.
[31] G. Yan, J.R. White, Polym. Eng. Sci. 39 (1999) 1866.
[32] J.H. Jou, L. Hsu, J. Appl. Phys. 76 (1994) 584.
[33] J.J. Barnes, J.G. Goedjen, D.A. Shores, Oxid. Met. 32 (1989) 449.
[34] S. Ko, D. Lee, S. Jee, H. Park, K. Lee, W. Hwang, Thin Solid Films 515 (2006) 1932.